

New effect in wave-packet scatterings of quantum fields: Saddle points, Lefschetz thimbles, and Stokes phenomenon

Kenzo Ishikawa,^{*} Kenji Nishiwaki,[†] and Kin-ya Oda[‡]

^{*} *Department of Physics, Hokkaido University, Hokkaido 060-0810, Japan*

^{*} *Research and Education Center for Natural Sciences, Keio University Kanagawa 223-8521, Japan*

[†] *Department of Physics, Shiv Nadar University, Gautam Buddha Nagar 201314, India*

[‡] *Department of Physics, Osaka University, Osaka 560-0043, Japan*

[‡] *Department of Mathematics, Tokyo Woman's Christian University, Tokyo 167-8585, Japan*

We find a new contribution in wave-packet scatterings, which has been overlooked in the standard formulation of S-matrix. As a concrete example, we consider a two-to-two scattering of light scalars ϕ by another intermediate heavy scalar Φ , in the Gaussian wave-packet formalism: $\phi\phi \rightarrow \Phi \rightarrow \phi\phi$. This contribution can be interpreted as an “in-time-boundary effect” of Φ for the corresponding $\Phi \rightarrow \phi\phi$ decay, proposed by Ishikawa et al., with a newly found modification that would cure the previously observed ultraviolet divergence. We show that such an effect can be understood as a Stokes phenomenon in an integral over complex energy plane: The number of relevant saddle points and Lefschetz thimbles (steepest descent paths) discretely changes depending on the configurations of initial and final states in the scattering.

INTRODUCTION

Particle scattering in quantum field theory requires wave packets in its very foundation, whereas the plane-wave formulation, which involves the square of energy-momentum delta function in S-matrix, is “more a mnemonic than a derivation” [1]. However, it has long been believed that there are no new phenomena arising from taking into account the wave-packet effects.

On the other hand, Ishikawa et al. claim that indeed a wave-packet effect—more specifically the *time-boundary effect* due to localization of wave-packet overlap in time—is responsible for diverse phenomena in science such as the LSND neutrino anomaly [2, 3]; violation of selection rules [4]; the solar coronal heating problem [5]; anomalous Thomson scattering and a speculative alternative to dark matter, as well as modified Haag theorem [6]; the anomalous excitation energy transfer in photosynthesis [7]; and anomalies in width in $e^+e^- \rightarrow \gamma\gamma$, in π^0 lifetime, in Raman scattering, and in the water vapor continuum absorption [8, 9]. There is an ongoing experimental project for this effect [8, 10].

However, the time-boundary effect has not been paid high attention, because so far it depends on whether one accepts *a priori* the concept of a finite-time scattering that yields the time-boundary effect (when combined with the localization of wave-packet overlap in time). Here, we fill the gap by proving existence of a new effect, which shares the same property as the time-boundary effect of a sub-process, even in an S-matrix with an infinite transition time.

Now we turn to more concrete backgrounds of this Let-

ter. The authors of Ref. [11] have proposed the Gaussian wave-packet formalism that fully takes advantage of the completeness of the Gaussian basis. Based on this formalism, it has been argued that one-to-two processes such as the scalar $\Phi \rightarrow \phi\phi$ decay have extra contributions arising from the in and out time-boundaries that are respectively the starting and end points of the transition [12].

In general, validity of the time-boundary effect depends [13, 14] on the assumption that the in and out wave-packet states can be well approximated by the free Gaussian states even when interactions are non-negligible there. Physically, the claimed in and out time-boundary effects would represent some yet unspecified production and detection processes of Φ and $\phi\phi$, respectively.

In this Letter, we study a $\phi\phi \rightarrow \Phi \rightarrow \phi\phi$ scattering without assuming any boundary effect of initial and final $\phi\phi$ states, and show existence of new contribution that share the same property as the in-boundary effect of $\Phi \rightarrow \phi\phi$. This is how we take into account the production process of Φ and resolve the in-boundary ambiguity for $\Phi \rightarrow \phi\phi$.

S-MATRIX IN GAUSSIAN FORMALISM

We consider the scattering $\phi\phi \rightarrow \Phi \rightarrow \phi\phi$ with an interaction Lagrangian density $\mathcal{L} = -\frac{\kappa}{2}\phi^2\Phi$, where ϕ and Φ are real scalar fields with masses m and M ($> 2m$), respectively, and κ is a coupling constant. We only take into account the tree-level *s*-channel scattering as we are mostly interested in amplitudes near the

resonance pole of Φ . Input parameters for each wave packet a (with $a = 1, 2$ for incoming and $3, 4$ for outgoing) are its width-squared σ_a , spacetime position of its center $X_a = (X_a^0, \mathbf{X}_a)$, and its central momentum $P_a = (E_a, \mathbf{P}_a)$, where $E_a := (m^2 + \mathbf{P}_a^2)^{1/2}$. We may trade \mathbf{P}_a for $\mathbf{V}_a := \mathbf{P}_a/E_a$ as independent parameters.

We write the plane-wave propagator of Φ with an off-shell momentum $p = (p^0, \mathbf{p})$ as $\frac{-i}{-(p^0)^2 + \mathbf{E}_p^2}$, where $\mathbf{E}_p := (E_p^2 - i\epsilon)^{1/2}$ with $E_p := (M^2 + \mathbf{p}^2)^{1/2} > \epsilon > 0$. Loop corrections to the two-point function of Φ may be approximated by taking $\epsilon = M\Gamma$, with Γ being the decay width of Φ [15]. In total, (κ, m, M, ϵ) and $(\sigma_a, X_a, \mathbf{P}_a)$ are all the independent parameters in this Letter: The former fixes the theory [16], while the latter parametrizes each wave packet a .

For the given Gaussian wave packets, $f_{\sigma_a; X_a, \mathbf{P}_a}$, the tree-level s -channel S-matrix \mathcal{S} is given as Eq. (42) in Ref. [14] with the limit $T_{\text{in}} \rightarrow -\infty$ and $T_{\text{out}} \rightarrow \infty$ [17]. We work at the leading order in the plane-wave expansion for large σ_a [11, 13, 14]. Then the eight-dimensional spacetime integral over the in- and out-interaction points becomes Gaussian, and the result is

$$\mathcal{S} = (2\pi)^4 (-i\kappa)^2 \left(\prod_{a=1}^4 \frac{1}{\sqrt{2E_a} (\pi\sigma_a)^{3/4}} \right) \sqrt{\sigma_{\text{in}}^3 \sigma_{\text{out}}^3 \varsigma_{\text{in}} \varsigma_{\text{out}}} \times \int \frac{d^4 p}{(2\pi)^4} \frac{-i}{p^2 + M^2 - i\epsilon} e^{F(p^0; \mathbf{p})}, \quad (1)$$

where $\sigma_{\text{in}} := \frac{\sigma_1 \sigma_2}{\sigma_1 + \sigma_2}$ and $\sigma_{\text{out}} := \frac{\sigma_3 \sigma_4}{\sigma_3 + \sigma_4}$ ($\varsigma_{\text{in}} = \frac{\sigma_1 + \sigma_2}{(\mathbf{V}_1 - \mathbf{V}_2)^2}$ and $\varsigma_{\text{out}} = \frac{\sigma_3 + \sigma_4}{(\mathbf{V}_3 - \mathbf{V}_4)^2}$) are the spatial (time-like) width-squared for the in and out interaction regions, respectively, and the exponent becomes quadratic in p^0 :

$$F(p^0; \mathbf{p}) = F_*(\mathbf{p}) - \frac{\varsigma_+}{2} (p^0 - p_*^0(\mathbf{p}))^2, \quad (2)$$

in which $\varsigma_+ := \varsigma_{\text{in}} + \varsigma_{\text{out}}$, $p_*^0(\mathbf{p}) = \Omega(\mathbf{p}) - i\frac{\delta\mathfrak{I}}{\varsigma_+}$, and $F_*(\mathbf{p})$ can be read off from Eq. (107) in Ref. [14] (its explicit form is mostly irrelevant for the following discussion; see Refs. [13, 14] for further notation; we have also prepared Supplemental Material. Physically, $\Omega(\mathbf{p})$ is the off-shell energy of Φ , and $\delta\mathfrak{I}$ is the time passed from the in-interaction to the out-interaction; see each Fig. 1 in Refs. [13, 14]. Both of them vary according to the wave packet configurations $(\sigma_a, X_a, \mathbf{P}_a)$.

SADDLE POINT

The second line in Eq. (1), a “wave-packet Feynman propagator”, may be written as $\int \frac{d^3 \mathbf{p}}{(2\pi)^3} e^{F_*(\mathbf{p})} I(\mathbf{p})$, where

$$I(\mathbf{p}) := \int_{-\infty}^{\infty} \frac{dp^0}{2\pi} \frac{-i}{-(p^0)^2 + \mathbf{E}_p^2} e^{-\frac{\varsigma_+}{2} (p^0 - p_*^0(\mathbf{p}))^2}. \quad (3)$$

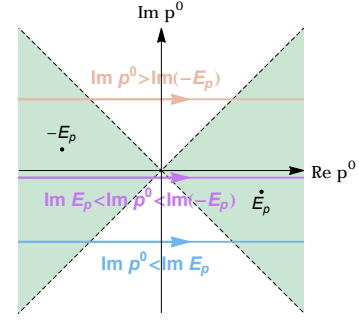


FIG. 1. Shaded region represents convergent directions $\Re F \rightarrow -\infty$ for $|p^0| \rightarrow \infty$. The points $\pm \mathbf{E}_p$ denote the poles of the propagator of Φ . The orange, purple, and blue lines represent the integral path of I_* in Eq. (4) for $\Im p^0 > \Im(-\mathbf{E}_p)$, $\Im \mathbf{E}_p < \Im p^0 < \Im(-\mathbf{E}_p)$, and $\Im p^0 < \Im \mathbf{E}_p$, respectively.

The exponential factor has a saddle point at $p^0 = p_*^0(\mathbf{p})$ with the steepest descent and ascent paths being $\Im(p^0 - p_*^0(\mathbf{p})) = 0$ and $\Re(p^0 - p_*^0(\mathbf{p})) = 0$, where \Re and \Im denote the real and imaginary parts, respectively. The saddle-point contribution is

$$I_*(\mathbf{p}) = \int_{-\infty + \Im p_*^0}^{\infty + \Im p_*^0} \frac{dp^0}{2\pi} \frac{-i}{-(p^0)^2 + \mathbf{E}_p^2} e^{-\frac{\varsigma_+}{2} (p^0 - p_*^0(\mathbf{p}))^2} \approx \frac{1}{\sqrt{2\pi\varsigma_+}} \frac{-i}{-(\Omega(\mathbf{p}) - i\frac{\delta\mathfrak{I}}{\varsigma_+})^2 + \mathbf{E}_p^2}, \quad (4)$$

which leads to Eq. (110) in Ref. [14]. The standard plane-wave result has been obtained by taking into account this contribution only, and no in-boundary effect for $\Phi \rightarrow \phi\phi$ has been found in the limit $\delta\mathfrak{I} \rightarrow 0$ [14].

The key observation in this Letter is that, as shown in Fig. 1, the saddle-point integral I_* over the steepest descent path from $-\infty + \Im p_*^0$ to $\infty + \Im p_*^0$ differs from I in Eq. (3) by the residue at the poles $p^0 = \mathbf{E}_p$ and $-\mathbf{E}_p$ when $\Im p^0 < \Im \mathbf{E}_p$ and $\Im p^0 > -\Im \mathbf{E}_p$, respectively:

$$I(\mathbf{p}) = I_*(\mathbf{p}) + \frac{e^{-\frac{\varsigma_+}{2} (\Omega(\mathbf{p}) - \mathbf{E}_p - i\frac{\delta\mathfrak{I}}{\varsigma_+})^2}}{2\mathbf{E}_p} \theta\left(\frac{\delta\mathfrak{I}}{\varsigma_+} + \Im \mathbf{E}_p\right) + \frac{e^{-\frac{\varsigma_+}{2} (\Omega(\mathbf{p}) + \mathbf{E}_p - i\frac{\delta\mathfrak{I}}{\varsigma_+})^2}}{2\mathbf{E}_p} \theta\left(\Im \mathbf{E}_p - \frac{\delta\mathfrak{I}}{\varsigma_+}\right), \quad (5)$$

where θ is the Heaviside step function. Eq. (5) is one of our main results. When ϵ is small, we have $\Im \mathbf{E}_p \simeq -\frac{\epsilon}{2E_p}$, and the second and third terms are non-zero when $\delta\mathfrak{I} > \frac{\epsilon\varsigma_+}{2E_p}$ and $\delta\mathfrak{I} < -\frac{\epsilon\varsigma_+}{2E_p}$, respectively; each of them corresponds to a configuration of wave packets that gives forward and backward propagation of Φ in time, respectively; see Fig. 1 in Ref. [14]. Note that, dropping the Heaviside function, the ratio of the second term to the third is $\exp(-2\varsigma_+ E_p p_*^0)$, and hence the third term is exponentially small when $\varsigma_+ E_p \Omega(\mathbf{p})$ is large.

The second term in Eq. (5) is the new contribution in addition to the ordinary $I_*(\mathbf{p})$. This term share

the same property with the in-time-boundary effect for $\Phi \rightarrow \phi\phi$ [14]: An exponential suppression $\exp[-\frac{(\delta\Im)^2}{2\varsigma_+}]$ that comes from $F_*(\mathbf{p})$ is cancelled by $\exp[\frac{(\delta\Im)^2}{2\varsigma_+}]$ from Eq. (5) for large $\delta\Im$, unlike the ordinary $I_*(\mathbf{p})$. Namely, the propagation of Φ in time is not exponentially suppressed by the passed time $\delta\Im$, which is a characteristic of the time-boundary effect: If it comes from the boundary, it does not matter how large is the bulk. Also, we newly find the extra suppression factor $\exp[-\frac{\varsigma_+}{2}(\Omega(\mathbf{p}) - \mathbf{E}_\mathbf{p})^2]$ in the second term in Eq. (5), which would cure the previously found possible ultraviolet divergence in the time-boundary contribution, related to energy-non-conserving configurations that are non-vanishing for $|\Omega(\mathbf{p}) - \mathbf{E}_\mathbf{p}| \rightarrow \infty$; see Sec. 4.3 in Ref. [13].

STOKES PHENOMENON

Here we show that the result (5) can be understood as a Stokes phenomenon. We first rewrite the integral (3) into an exponential form: $I(\mathbf{p}) = \int_{-\infty}^{\infty} \frac{dp^0}{2\pi i} e^{\mathcal{F}(p^0; \mathbf{p})}$, where

$$\mathcal{F}(p^0) = -\frac{\varsigma_+}{2} (p^0 - p_*^0)^2 - \ln\left(-(p^0)^2 + \mathbf{E}_\mathbf{p}^2\right). \quad (6)$$

Here and hereafter, we drop the \mathbf{p} -dependence and write $\mathcal{F}(p^0)$ etc. for simplicity.

By solving $\frac{\partial \mathcal{F}}{\partial p^0} = 0$, we obtain the following three saddle points:

$$p_{(*)}^0 = p_*^0 + \frac{1}{\varsigma_+} \frac{2p_*^0}{-(p_*^0)^2 + \mathbf{E}_\mathbf{p}^2} + \dots, \quad (7)$$

$$p_{(\pm)}^0 = \pm \mathbf{E}_\mathbf{p} + \frac{1}{\varsigma_+} \frac{1}{p_*^0 \mp \mathbf{E}_\mathbf{p}} + \dots, \quad (8)$$

with

$$\mathcal{F}_{(*)} = \ln \frac{1}{-(p_*^0)^2 + \mathbf{E}_\mathbf{p}^2} + \frac{1}{\varsigma_+} \frac{2(p_*^0)^2}{((p_*^0)^2 - \mathbf{E}_\mathbf{p}^2)^2} + \dots, \quad (9)$$

$$\mathcal{F}_{(\pm)} = -\frac{\varsigma_+}{2} (p_*^0 \mp \mathbf{E}_\mathbf{p})^2 + \ln\left(\frac{\varsigma_+}{2} \left(1 \mp \frac{p_*^0}{\mathbf{E}_\mathbf{p}}\right)\right) + 1 + \dots, \quad (10)$$

and

$$\frac{\partial^2 \mathcal{F}_{(*)}}{\partial p^{02}} = -\varsigma_+ + \frac{1}{(p_*^0 + \mathbf{E}_\mathbf{p})^2} + \frac{1}{(p_*^0 - \mathbf{E}_\mathbf{p})^2} + \dots, \quad (11)$$

$$\frac{\partial^2 \mathcal{F}_{(\pm)}}{\partial p^{02}} = \varsigma_+^2 (p_*^0 \mp \mathbf{E}_\mathbf{p})^2 - \left(2 \pm \frac{p_*^0}{\mathbf{E}_\mathbf{p}}\right) \varsigma_+ + \dots, \quad (12)$$

where we have included up to the sub-leading terms (as well as the order- $\ln \varsigma_+$ term) for large ς_+ [18].

For each saddle point (i) with $i = *$ and \pm , the steepest decent and ascent paths are obtained from the condition $\Im(\mathcal{F}(p^0) - \mathcal{F}_{(i)}) = 0$. The steepest descent path

$\mathcal{J}_{(i)}$ (ascent path $\mathcal{K}_{(i)}$) from the saddle point (i) is called the Lefschetz thimble or the Stokes line (the anti-thimble or the anti-Stokes line). Along $\mathcal{J}_{(i)}$, we may evaluate the approximate Gaussian integral $I_{(i)} = \int_{\mathcal{J}_{(i)}} \frac{dp^0}{2\pi i} e^{\mathcal{F}(p^0)}$ without the oscillation of integrand:

$$I_{(*)} \simeq \frac{1}{\sqrt{2\pi\varsigma_+ - (p_*^0)^2 + \mathbf{E}_\mathbf{p}^2}} \frac{-i}{\sqrt{2\pi}} \frac{e^{-\frac{\varsigma_+}{2}(p_*^0 \mp \mathbf{E}_\mathbf{p})^2}}{2\mathbf{E}_\mathbf{p}}. \quad (13)$$

The integral I can be decomposed into those on the Lefschetz thimbles:

$$I = \sum_{i=*, \pm} \langle \mathcal{K}_{(i)}, \mathbb{R} \rangle I_{(i)}, \quad (14)$$

where $\langle \mathcal{K}_{(i)}, \mathbb{R} \rangle$ is the intersection number between the anti-thimble $\mathcal{K}_{(i)}$ and the original integration path \mathbb{R} ; see e.g. Ref. [19] for a review. We see that the result (5) is reproduced under the saddle-point approximation up to the extra factor $\frac{e}{\sqrt{2\pi}} \simeq 1.08$.

In Fig. 2, we plot $e^{\Re \mathcal{F}}$ in the first panel, while in others, we show contours for $\Im \mathcal{F} \pmod{2\pi}$ on a density plot of $\Re \mathcal{F}$; see the caption for more details.

In each panel for $\Im \mathcal{F}$, through the saddle point $p_{(*)}^0$, the horizontal and vertical contours (red-solid) are the thimble $\mathcal{J}_{(*)}$ and the anti-thimble $\mathcal{K}_{(*)}$, respectively. On the other hand, through the saddle point $p_{(+) }^0$, the yellow-dashed contour that connects $\mathbf{E}_\mathbf{p}$ and a $|\Im p^0| \rightarrow \infty$ region is the anti-thimble $\mathcal{K}_{(+)}$, while its perpendicular contour is the thimble $\mathcal{J}_{(+)}$. Similarly, through $p_{(-)}^0$, the green-dotted contour connecting $-\mathbf{E}_\mathbf{p}$ and a $|\Im p^0| \rightarrow \infty$ region is $\mathcal{K}_{(-)}$, and its perpendicular, $\mathcal{J}_{(-)}$. All the other contours that are disconnected from any of $p_{(i)}^0$ are irrelevant for the integral.

We comment on the branch cuts for the logarithmic function in Eq. (6). In the case $\Im p_{(*)}^0 \lesssim \Im \mathbf{E}_\mathbf{p}$ in the second panel, we may put a branch cut from $-\mathbf{E}_\mathbf{p}$ to $-\infty + \Im(-\mathbf{E}_\mathbf{p})$ and another from $\mathbf{E}_\mathbf{p}$ along a, say, red-solid or green-dotted contour. This way, we may continuously deform \mathbb{R} into the thimbles $\mathcal{J}_{(*)}$ and $\mathcal{J}_{(+)}$ without crossing the cuts. It is obvious that we may do similarly for other cases. In Fig. 3, we further explain artifact lines due to the branch cuts in the numerical computation.

There are three cases depending on the relative position of $\mathcal{J}_{(*)}$ and $\pm \mathbf{E}_\mathbf{p}$, represented by the last three panels in Fig. 2. When $\Im p_{(*)}^0 \lesssim \Im \mathbf{E}_\mathbf{p}$, we see in the second panel (as magnified in Fig. 3) that the anti-thimbles $\mathcal{K}_{(-)}$ (green-dotted) terminate in $-\mathbf{E}_\mathbf{p}$, and hence do not intersect with the real axis: $\langle \mathcal{K}_{(-)}, \mathbb{R} \rangle = 0$. Similarly when $\Im p_{(*)}^0 \gtrsim \Im(-\mathbf{E}_\mathbf{p})$, in the fourth panel, $\mathcal{K}_{(+)}$ (yellow-dashed) terminate in $\mathbf{E}_\mathbf{p}$, and hence $\langle \mathcal{K}_{(+)}, \mathbb{R} \rangle = 0$. When $\Im \mathbf{E}_\mathbf{p} \lesssim \Im p_{(*)}^0 \lesssim \Im(-\mathbf{E}_\mathbf{p})$, in the third panels, both anti-thimbles terminate in $\pm \mathbf{E}_\mathbf{p}$, and hence $\langle \mathcal{K}_{(\pm)}, \mathbb{R} \rangle = 0$. This is how the discrete change in the amplitude (5) is understood as a Stokes phenomenon in Eq. (14).

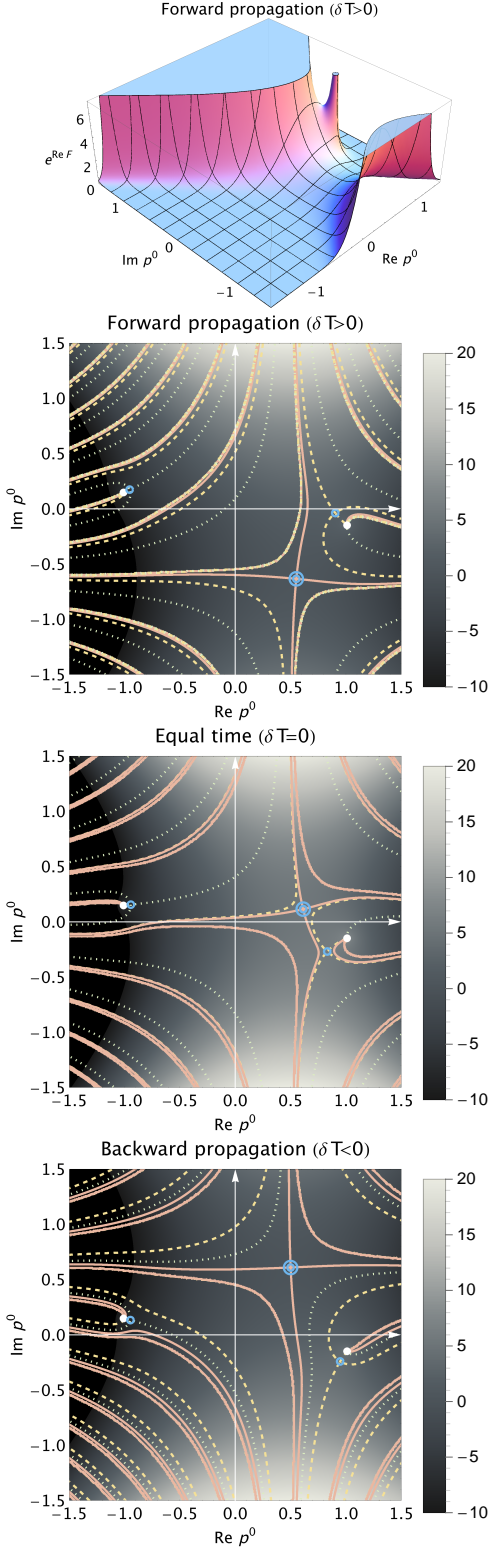


FIG. 2. In the first panel, we plot $e^{\Re \mathcal{F}}$, whereas in the other three, we show contours for $\Im \mathcal{F} \pmod{2\pi}$, on a density plot of $\Re \mathcal{F}$ in $[-10, 20]$. We have chosen sample parameters $\varsigma_+ = 10$, $\Omega (= \Re p_*^0) = 5$, and $\epsilon = 0.3$ in the $E_{\mathbf{p}} = 1$ units. Both the first and second panels correspond to forward propagation of Φ with $\frac{\delta \Im}{\varsigma_+} (= -\Im p_*^0) = 0.5$, while the third and fourth to equal-time and backward with $\frac{\delta \Im}{\varsigma_+} = 0$ and -0.5 , respectively. The red-solid, yellow-dashed, and green-dotted contours are $\Im \mathcal{F} = \Im \mathcal{F}_*$, $\Im \mathcal{F}_+$, and $\Im \mathcal{F}_-$ respectively. The white dots denote the poles at $p^0 = \pm E_{\mathbf{p}}$ and the blue single circles nearby them are correspondingly the saddle points $p_{(\pm)}^0$. The blue double circle denote the saddle point $p_{(*)}^0$.

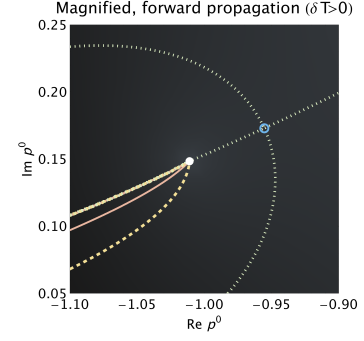


FIG. 3. Magnified plot for $\Im \mathcal{F} \pmod{2\pi}$ of the second panel in Fig. 2 near the saddle point $p_{(-)}^0$ (blue circle) and the pole $-E_{\mathbf{p}}$ (white dot). We see that three contours and an artifact line terminate in $-E_{\mathbf{p}}$: The three contours are $\Im \mathcal{F} = \Im \mathcal{F}_*$ (red-solid), $\Im \mathcal{F} = \Im \mathcal{F}_+$ (yellow-dashed), and especially the anti-thimble $\mathcal{K}_{(-)}$ (green-dotted) from $p_{(-)}^0$. The extra artifact line, seemingly consisting of three degenerate contours, is from a branch cut of logarithmic function in the numerical computation, along which contributions from all the other Riemann surfaces appear. This way, in each pole in Fig. 2, there always terminate three contours and an artifact line.

SUMMARY AND DISCUSSION

We have studied the wave-packet scattering $\phi\phi \rightarrow \Phi \rightarrow \phi\phi$ within the infinite time interval and hence without any time-boundary effect for ϕ . We have obtained the new contribution that shares the same property as the in-time-boundary effect for $\Phi \rightarrow \phi\phi$. The appearance of this effect is consistently understood as the Stokes phenomenon.

This effect is intrinsically absent in the plane-wave S-matrix. Note that the Wick rotation from $\mathcal{J}_{(*)}$ to $\mathcal{K}_{(*)}$ makes the p^0 -integral exponentially divergent.

In this Letter, we have integrated over the times of interaction before p^0 . Instead we may first integrate over p^0 before them, in which all the exponents are linear in p^0 and the Wick rotation is allowed, and confirm that the time-boundary effect emerges at the time-boundaries $\mathfrak{T}_{\text{in/out}}$. This will be presented in detail in a separate publication.

It would be interesting to pursue the deviation $e/\sqrt{2\pi} \simeq 1.08$ between the residue computation and the saddle-point approximation. This factor does not depend on any physical parameter, and there may be mathematical account for it. In the case, say, $\Im p_{(*)}^0 \lesssim \Im E_{\mathbf{p}}$, in the plane-wave limit $\varsigma_+ \rightarrow \infty$, the saddle-point $p_{(+)}^0$ becomes closer and closer to the pole $E_{\mathbf{p}}$, and hence the thimble $\mathcal{J}_{(+)}$ becomes more and more curved near the pole. This might be a cause of the deviation of the approximate Gaussian integral along the straight line that is tangent to the curve.

Acknowledgement: We thank Osamu Jinnouchi for useful discussion and Juntaro Wada for reading the

manuscript. The work of K.O. is in part supported by JSPS Kakenhi Grant No. 19H01899.

-
- [1] S. Weinberg, *The Quantum theory of fields. Vol. 1: Foundations* (Cambridge University Press, 2005).
 - [2] K. Ishikawa and Y. Tobita, Resolving LSND Anomaly by Neutrino Diffraction, (2011), arXiv:1109.3105 [hep-ph].
 - [3] K. Ishikawa and Y. Tobita, Matter-enhanced transition probabilities in quantum field theory, *Annals Phys.* **344**, 118 (2014), arXiv:1206.2593 [hep-ph].
 - [4] K. Ishikawa, T. Tajima, and Y. Tobita, Anomalous radiative transitions, *PTEP* **2015**, 013B02 (2015), arXiv:1409.4339 [hep-ph].
 - [5] K. Ishikawa and Y. Tobita, Electroweak Hall Effect of Neutrino and Coronal Heating, (2015), arXiv:1503.07285 [hep-ph].
 - [6] K. Ishikawa and Y. Tobita, Finite-size corrections to Fermi's Golden rule II: Quasi-stationary composite states, (2016), arXiv:1607.08522 [hep-ph].
 - [7] N. Maeda, T. Yabuki, Y. Tobita, and K. Ishikawa, Finite-size corrections to the excitation energy transfer in a massless scalar interaction model, *PTEP* **2017**, 053J01 (2017), arXiv:1609.00160 [physics.chem-ph].
 - [8] K. Ishikawa, O. Jinnouchi, A. Kubota, T. Sloan, T. H. Tatsuishi, and R. Ushioda, On experimental confirmation of the corrections to Fermi's golden rule, *PTEP* **2019**, 033B02 (2019), arXiv:1901.03019 [hep-ph].
 - [9] K. Ishikawa, *Implications of the correction to the Fermi's golden rule*, in VIII · LA PARTE Y EL TODO: Workshop on advanced topics on high-energy physics and gravitation—Online via Zoom, Afunahue, Villarrica, Chile, 4–8 January 2021, https://laparteyeltodo.files.wordpress.com/2021/01/kishikawa_chille.pdf, .
 - [10] R. Ushioda, O. Jinnouchi, K. Ishikawa, and T. Sloan, Search for the correction term to the Fermi's golden rule in positron annihilation, *PTEP* **2020**, 043C01 (2020), arXiv:1907.01264 [hep-ex].
 - [11] K. Ishikawa and T. Shimomura, Generalized S-matrix in mixed representations, *Prog. Theor. Phys.* **114**, 1201 (2006), arXiv:hep-ph/0508303 [hep-ph].
 - [12] K. Ishikawa and Y. Tobita, Finite-size corrections to Fermi's golden rule: I. Decay rates, *PTEP* **2013**, 073B02 (2013), arXiv:1303.4568 [hep-ph].
 - [13] K. Ishikawa and K.-Y. Oda, Particle decay in Gaussian wave-packet formalism revisited, *PTEP* **2018**, 123B01 (2018), arXiv:1809.04285 [hep-ph].
 - [14] K. Ishikawa, K. Nishiwaki, and K.-y. Oda, Scalar scattering amplitude in the Gaussian wave-packet formalism, *PTEP* **2020**, 103B04 (2020), arXiv:2006.14159 [hep-th].
 - [15] See e.g. Appendix C and D in Ref. [20] and references therein, for subtleties when Γ becomes comparable to M .
 - [16] Within this particular theory, ϵ is not an independent variable as it can be computed for a given set of parameters (κ, m, M) . Here it is left independent for ease of extension.
 - [17] In this Letter, we first *neglect* the time-boundary effects of ϕ ; focus on the “bulk effect” [14] for $\phi\phi \rightarrow \Phi \rightarrow \phi\phi$; and then show that the in-time-boundary effect of Φ for $\Phi \rightarrow \phi\phi$ still *emerges*.
 - [18] The saddle-point equation is cubic in p^0 , and we obtain exact solutions for $p_{(i)}^0$. Here we show the large- ς_+ results as an illustration, though we use the exact ones in the following numerical plots.
 - [19] Y. Tanizaki, *Study on sign problem via Lefschetz-thimble path integral*, https://ribf.riken.jp/~tanizaki/thesis/yuya_phd.pdf, Ph.D. thesis, Tokyo U. (2015).
 - [20] K. Nishiwaki, K.-y. Oda, N. Okuda, and R. Watanabe, Heavy Higgs at Tevatron and LHC in Universal Extra Dimension Models, *Phys. Rev. D* **85**, 035026 (2012), arXiv:1108.1765 [hep-ph].

SUPPLEMENTAL MATERIAL

Here we provide more detailed expressions that are omitted in the main text. These are not necessary to follow it but may be useful.

S-MATRIX IN GAUSSIAN FORMALISM

We write the plane-wave propagator of Φ :

$$\frac{-i}{p^2 + M^2 - i\epsilon} = \frac{-i}{-(p^0)^2 + \mathbf{p}^2 + M^2 - i\epsilon} = \frac{-i}{-(p^0)^2 + E_{\mathbf{p}}^2 - i\epsilon} = \frac{-i}{-(p^0)^2 + \mathbf{E}_{\mathbf{p}}^2}, \quad (15)$$

where $E_{\mathbf{p}} := \sqrt{M^2 + \mathbf{p}^2}$ and $\mathbf{E}_{\mathbf{p}} := \sqrt{E_{\mathbf{p}}^2 - i\epsilon}$.

For given Gaussian wave packets, $f_{\sigma_a; X_a, \mathbf{P}_a}$, the tree-level s -channel S-matrix reads [14]

$$\mathcal{S} = (-i\kappa)^2 \int \frac{d^4 p}{(2\pi)^4} \frac{-i}{p^2 + M^2 - i\epsilon} \int d^4 x f_{\sigma_1; X_1, \mathbf{P}_1}(x) f_{\sigma_2; X_2, \mathbf{P}_2}(x) e^{-ip \cdot x} \int d^4 y f_{\sigma_3; X_3, \mathbf{P}_3}^*(y) f_{\sigma_4; X_4, \mathbf{P}_4}^*(y) e^{ip \cdot y}, \quad (16)$$

where the exponential factors come from the plane-wave expansion of Φ , and we integrate for the spacetime position of “in-interaction” x and that of “out-interaction” y . The result does not differ if we expand Φ by the Gaussian waves instead of the plane waves [14].

In principle, there can be a “time-boundary effect” of ϕ for each a at the time X_a^0 . As said in the main text, we neglect them. In order to get the bulk effect, we could have introduced time boundaries for the two-to-two scattering, T_{in} and T_{out} , at which interactions are negligible; have cut off the interaction-time integrals $\int_{T_{\text{in}}}^{T_{\text{out}}} dx^0$ and $\int_{T_{\text{in}}}^{T_{\text{out}}} dy^0$; have focused on the “bulk terms”; and have taken $T_{\text{in}} \rightarrow -\infty$ and $T_{\text{out}} \rightarrow \infty$.

We work at the leading order in the plane-wave expansion for large σ_a [11, 13, 14]:

$$f_{\sigma_a; X_a, \mathbf{P}_a}(z) \simeq \frac{e^{iP_a \cdot (z - X_a)}}{(\pi\sigma)^{3/4} \sqrt{2E_a}} e^{-\frac{1}{2\sigma_a} [z - \mathbf{X}_a - (z^0 - X_a^0) \mathbf{V}_a]^2}. \quad (17)$$

Then all the exponents in \mathcal{S} become quadratic in x and y , and we may perform the eight-dimensional Gaussian integral to get the form

$$\mathcal{S} = (2\pi)^4 (-i\kappa)^2 \left(\prod_{a=1}^4 \frac{1}{\sqrt{2E_a} (\pi\sigma_a)^{3/4}} \right) \sqrt{\sigma_{\text{in}}^3 \sigma_{\text{out}}^3 \varsigma_{\text{in}} \varsigma_{\text{out}}} \int \frac{d^4 p}{(2\pi)^4} \frac{-i}{p^2 + M^2 - i\epsilon} e^{F(p^0; \mathbf{p})}, \quad (18)$$

where $\sigma_{\text{in}} := \frac{\sigma_1 \sigma_2}{\sigma_1 + \sigma_2}$ and $\sigma_{\text{out}} := \frac{\sigma_3 \sigma_4}{\sigma_3 + \sigma_4}$ ($\varsigma_{\text{in}} = \frac{\sigma_1 + \sigma_2}{(\mathbf{V}_1 - \mathbf{V}_2)^2}$ and $\varsigma_{\text{out}} = \frac{\sigma_3 + \sigma_4}{(\mathbf{V}_3 - \mathbf{V}_4)^2}$) are the spatial (time-like) width-squared for the in and out interaction regions, respectively; see Refs. [13, 14] for further details.

We also show expressions for $\sigma_1 = \sigma_2 = \sigma_3 = \sigma_4 (=:\mathbf{s})$ after “ \rightsquigarrow ” as an illustration: $\sigma_{\text{in}} \rightsquigarrow \frac{\mathbf{s}}{2}$, $\sigma_{\text{out}} \rightsquigarrow \frac{\mathbf{s}}{2}$, $\varsigma_{\text{in}} \rightsquigarrow \frac{2\mathbf{s}}{(\mathbf{V}_1 - \mathbf{V}_2)^2}$, $\varsigma_{\text{out}} \rightsquigarrow \frac{2\mathbf{s}}{(\mathbf{V}_3 - \mathbf{V}_4)^2}$, and

$$\mathcal{S} \rightsquigarrow \frac{(-i\kappa)^2 \pi \mathbf{s}}{\sqrt{E_1 E_2} |\mathbf{V}_1 - \mathbf{V}_2| \sqrt{E_3 E_4} |\mathbf{V}_3 - \mathbf{V}_4|} \int \frac{d^4 p}{(2\pi)^4} \frac{-i}{p^2 + M^2 - i\epsilon} e^{F(p^0; \mathbf{p})}. \quad (19)$$

Note that a head-on collision in the center-of-mass frame corresponds to $\mathbf{V}_1 + \mathbf{V}_2 = 0$ and, further in the massless limit $m \rightarrow 0$, to $|\mathbf{V}_1 - \mathbf{V}_2| \rightarrow 2$.

Originally, the exponents in Eq. (16) are linear in p^0 . After the Gaussian integral over x and y , the exponents in Eq. (18) become quadratic in p^0 :

$$F(p^0; \mathbf{p}) = F_*(\mathbf{p}) - \frac{\varsigma_+}{2} (p^0 - p_*^0(\mathbf{p}))^2, \quad (20)$$

where $\varsigma_+ := \varsigma_{\text{in}} + \varsigma_{\text{out}}$. The location of saddle point $p_*^0(\mathbf{p})$ in the complex p^0 plane becomes

$$p_*^0(\mathbf{p}) = \Omega(\mathbf{p}) - i \frac{\delta \Im}{\varsigma_+}, \quad (21)$$

where we define a wave-average of (what-we-call) “wave-packet kinetic energies”, $\Omega(\mathbf{p})$, and the time difference between the in and out interactions, $\delta\mathfrak{T}$,

$$\Omega(\mathbf{p}) := \frac{\varsigma_{\text{in}}\omega_{\text{in}}(\mathbf{p}) + \varsigma_{\text{out}}\omega_{\text{out}}(\mathbf{p})}{\varsigma_{\text{in}} + \varsigma_{\text{out}}} \rightsquigarrow \frac{\frac{\omega_{\text{in}}(\mathbf{p})}{(\mathbf{V}_1 - \mathbf{V}_2)^2} + \frac{\omega_{\text{out}}(\mathbf{p})}{(\mathbf{V}_3 - \mathbf{V}_4)^2}}{\frac{1}{(\mathbf{V}_1 - \mathbf{V}_2)^2} + \frac{1}{(\mathbf{V}_3 - \mathbf{V}_4)^2}}, \quad (22)$$

$$\delta\mathfrak{T} := \mathfrak{T}_{\text{out-int}} - \mathfrak{T}_{\text{in-int}}, \quad (23)$$

in which we use the following notations:

- $\Xi_a := \mathbf{X}_a - \mathbf{V}_a X_a^0$ denotes the spatial center of each wave packet a at a reference time $t = 0$. (In Refs. [13, 14], Ξ_a has been written as \mathfrak{X}_a .)
- The wave-packet kinetic energies are

$$\omega_{\text{in}}(\mathbf{p}) := E_{\text{in}} + \bar{\mathbf{V}}_{\text{in}} \cdot (\mathbf{p} - \mathbf{P}_{\text{in}}) \rightsquigarrow E_{\text{in}} + \frac{\mathbf{V}_1 + \mathbf{V}_2}{2} \cdot (\mathbf{p} - \mathbf{P}_{\text{in}}), \quad (24)$$

$$\omega_{\text{out}}(\mathbf{p}) := E_{\text{out}} + \bar{\mathbf{V}}_{\text{out}} \cdot (\mathbf{p} - \mathbf{P}_{\text{out}}) \rightsquigarrow E_{\text{out}} + \frac{\mathbf{V}_3 + \mathbf{V}_4}{2} \cdot (\mathbf{p} - \mathbf{P}_{\text{out}}), \quad (25)$$

where $E_{\text{in}} := E_1 + E_2$ and $E_{\text{out}} := E_3 + E_4$ ($\mathbf{P}_{\text{in}} := \mathbf{P}_1 + \mathbf{P}_2$ and $\mathbf{P}_{\text{out}} := \mathbf{P}_3 + \mathbf{P}_4$) are the incoming and outgoing energies (momenta), respectively, and

$$\bar{\mathbf{V}}_{\text{in}} := \frac{\sigma_1\sigma_2}{\sigma_1 + \sigma_2} \left(\frac{\mathbf{V}_1}{\sigma_1} + \frac{\mathbf{V}_2}{\sigma_2} \right) \rightsquigarrow \frac{\mathbf{V}_1 + \mathbf{V}_2}{2}, \quad (26)$$

$$\bar{\mathbf{V}}_{\text{out}} := \frac{\sigma_3\sigma_4}{\sigma_3 + \sigma_4} \left(\frac{\mathbf{V}_3}{\sigma_3} + \frac{\mathbf{V}_4}{\sigma_4} \right) \rightsquigarrow \frac{\mathbf{V}_3 + \mathbf{V}_4}{2} \quad (27)$$

are the wave-averaged in and out velocities.

- The in- and out-interaction times are given by

$$\mathfrak{T}_{\text{in-int}} = -\frac{(\mathbf{V}_1 - \mathbf{V}_2) \cdot (\Xi_1 - \Xi_2)}{(\mathbf{V}_1 - \mathbf{V}_2)^2}, \quad (28)$$

$$\mathfrak{T}_{\text{out-int}} = -\frac{(\mathbf{V}_3 - \mathbf{V}_4) \cdot (\Xi_3 - \Xi_4)}{(\mathbf{V}_3 - \mathbf{V}_4)^2}. \quad (29)$$

The initial $\phi\phi$ wave packets intersect each other at $\mathfrak{T}_{\text{in-int}}$, and the final $\phi\phi$ at $\mathfrak{T}_{\text{out-int}}$.

The exponent at saddle point $F_*(\mathbf{p})$ is

$$F_*(\mathbf{p}) = \left(-\frac{\mathcal{R}_{\text{in}}}{2} - \frac{\sigma_{\text{in}}}{2} (\mathbf{p} - \mathbf{P}_{\text{in}})^2 - i\bar{\Xi}_{\text{in}} \cdot (\mathbf{p} - \mathbf{P}_{\text{in}}) \right) + \left(-\frac{\mathcal{R}_{\text{out}}}{2} - \frac{\sigma_{\text{out}}}{2} (\mathbf{p} - \mathbf{P}_{\text{out}})^2 + i\bar{\Xi}_{\text{out}} \cdot (\mathbf{p} - \mathbf{P}_{\text{out}}) \right) - \frac{(\delta\mathfrak{T})^2}{2\varsigma_+} + i\varsigma \left(\frac{\mathfrak{T}_{\text{in}}}{\varsigma_{\text{in}}} + \frac{\mathfrak{T}_{\text{out}}}{\varsigma_{\text{out}}} \right) \delta\omega(\mathbf{p}) - \frac{\varsigma}{2} (\delta\omega(\mathbf{p}))^2, \quad (30)$$

where $\varsigma := \frac{\varsigma_{\text{in}}\varsigma_{\text{out}}}{\varsigma_{\text{in}} + \varsigma_{\text{out}}}$ is a wave-average of the time-like width-squared; $\delta\omega(\mathbf{p}) := \omega_{\text{out}}(\mathbf{p}) - \omega_{\text{in}}(\mathbf{p})$ is the difference of the wave-packet kinetic energies; the wave-averaged position for the initial $\phi\phi$ (at the reference time $t = 0$) and that for the final $\phi\phi$ are

$$\bar{\Xi}_{\text{in}} = \frac{\sigma_1\sigma_2}{\sigma_1 + \sigma_2} \left(\frac{\Xi_1}{\sigma_1} + \frac{\Xi_2}{\sigma_2} \right) \rightsquigarrow \frac{\Xi_1 + \Xi_2}{2}, \quad (31)$$

$$\bar{\Xi}_{\text{out}} = \frac{\sigma_3\sigma_4}{\sigma_3 + \sigma_4} \left(\frac{\Xi_3}{\sigma_3} + \frac{\Xi_4}{\sigma_4} \right) \rightsquigarrow \frac{\Xi_3 + \Xi_4}{2}; \quad (32)$$

and the “overlap exponents” for the initial $\phi\phi$ wave packets and for the final $\phi\phi$ are, respectively,

$$\mathcal{R}_{\text{in}} = \frac{(\Xi_1 - \Xi_2)^2 + [\hat{\mathbf{V}}_{12} \cdot (\Xi_1 - \Xi_2)]^2}{\sigma_1 + \sigma_2}, \quad (33)$$

$$\mathcal{R}_{\text{out}} = \frac{(\Xi_3 - \Xi_4)^2 + [\hat{\mathbf{V}}_{34} \cdot (\Xi_3 - \Xi_4)]^2}{\sigma_3 + \sigma_4}, \quad (34)$$

in which $\hat{\mathbf{V}}_{12} := \frac{\mathbf{V}_1 - \mathbf{V}_2}{|\mathbf{V}_1 - \mathbf{V}_2|}$ and $\hat{\mathbf{V}}_{34} := \frac{\mathbf{V}_3 - \mathbf{V}_4}{|\mathbf{V}_3 - \mathbf{V}_4|}$.

SADDLE POINT

We compute a “wave-packet Feynman propagator”:

$$\int \frac{d^4 p}{(2\pi)^4} \frac{-i}{p^2 + M^2 - i\epsilon} e^{F(p^0; \mathbf{p})} = \int \frac{d^3 \mathbf{p}}{(2\pi)^3} e^{F_*(\mathbf{p})} I(\mathbf{p}), \quad (35)$$

where

$$I(\mathbf{p}) := \int_{-\infty}^{\infty} \frac{dp^0}{2\pi} \frac{-i}{-(p^0)^2 + \mathbf{E}_{\mathbf{p}}^2} e^{-\frac{\varsigma_{\pm}}{2} (p^0 - p_*^0(\mathbf{p}))^2}. \quad (36)$$

The key observation is that the saddle-point integral I_* over the steepest descent path from $-\infty + \Im p_*^0(\mathbf{p})$ to $\infty + \Im p_*^0(\mathbf{p})$ differs from the integral I over \mathbb{R} by the residues:

$$\begin{aligned} I(\mathbf{p}) &= I_*(\mathbf{p}) - \left(\text{Res}_{p^0 = \mathbf{E}_{\mathbf{p}}} \frac{e^{-\frac{\varsigma_{\pm}}{2} (p^0 - p_*^0(\mathbf{p}))^2}}{-(p^0)^2 + \mathbf{E}_{\mathbf{p}}^2} \right) \theta(\Im \mathbf{E}_{\mathbf{p}} - \Im p_*^0) + \left(\text{Res}_{p^0 = -\mathbf{E}_{\mathbf{p}}} \frac{e^{-\frac{\varsigma_{\pm}}{2} (p^0 - p_*^0(\mathbf{p}))^2}}{-(p^0)^2 + \mathbf{E}_{\mathbf{p}}^2} \right) \theta(\Im p_*^0 - \Im(-\mathbf{E}_{\mathbf{p}})) \\ &= I_*(\mathbf{p}) + \frac{e^{-\frac{\varsigma_{\pm}}{2} (\Omega(\mathbf{p}) - \mathbf{E}_{\mathbf{p}} - i\frac{\delta\Im}{\varsigma_{\pm}})^2}}{2\mathbf{E}_{\mathbf{p}}} \theta\left(\frac{\delta\Im}{\varsigma_{\pm}} + \Im \mathbf{E}_{\mathbf{p}}\right) + \frac{e^{-\frac{\varsigma_{\pm}}{2} (\Omega(\mathbf{p}) + \mathbf{E}_{\mathbf{p}} - i\frac{\delta\Im}{\varsigma_{\pm}})^2}}{2\mathbf{E}_{\mathbf{p}}} \theta\left(\Im \mathbf{E}_{\mathbf{p}} - \frac{\delta\Im}{\varsigma_{\pm}}\right). \end{aligned} \quad (37)$$

STOKES PHENOMENON

We first rewrite the integral (36) into an exponential form:

$$I(\mathbf{p}) = \int_{-\infty}^{\infty} \frac{dp^0}{2\pi i} e^{\mathcal{F}(p^0; \mathbf{p})}, \quad (38)$$

where

$$\mathcal{F}(p^0; \mathbf{p}) = -\frac{\varsigma_{\pm}}{2} (p^0 - p_*^0(\mathbf{p}))^2 - \ln\left(-(p^0)^2 + \mathbf{E}_{\mathbf{p}}^2\right). \quad (39)$$

We take the direction of $\mathcal{J}_{(\pm)}$ such that it can be deformed to \mathbb{R} without crossing the poles, namely, $\mathcal{J}_{(+)}$ and $\mathcal{J}_{(-)}$ circulate around $\mathbf{E}_{\mathbf{p}}$ and $-\mathbf{E}_{\mathbf{p}}$ clockwise and counterclockwise, respectively. Along $\mathcal{J}_{(i)}$, we may evaluate the approximate Gaussian integral

$$I_{(i)}(\mathbf{p}) = \int_{\mathcal{J}_{(i)}} \frac{dp^0}{2\pi i} e^{\mathcal{F}(p^0; \mathbf{p})} \quad (40)$$

without the oscillation of integrand:

$$I_{(*)}(\mathbf{p}) \simeq \frac{1}{\sqrt{2\pi\varsigma_{\pm}}} \frac{-i}{-(p_*^0(\mathbf{p}))^2 + \mathbf{E}_{\mathbf{p}}^2}, \quad (41)$$

$$I_{(\pm)}(\mathbf{p}) \simeq \mp \frac{-i}{\sqrt{2\pi}} \frac{1}{\sqrt{-\varsigma_{\pm}^2 (p_*^0(\mathbf{p}) \mp \mathbf{E}_{\mathbf{p}})^2}} e^{-\frac{\varsigma_{\pm}}{2} (p_*^0(\mathbf{p}) \mp \mathbf{E}_{\mathbf{p}})^2 + 1} \frac{\varsigma_{\pm}}{2} \left(1 \mp \frac{p_*^0(\mathbf{p})}{\mathbf{E}_{\mathbf{p}}}\right) = \frac{e}{\sqrt{2\pi}} \frac{e^{-\frac{\varsigma_{\pm}}{2} (p_*^0(\mathbf{p}) \mp \mathbf{E}_{\mathbf{p}})^2}}{2\mathbf{E}_{\mathbf{p}}}, \quad (42)$$

where we have taken $\sqrt{re^{i\theta}} = \sqrt{r}e^{i\theta/2}$ for $-\pi < \theta < \pi$, namely, $\sqrt{(p_*^0(\mathbf{p}) \mp \mathbf{E}_{\mathbf{p}})^2} = \mathbf{E}_{\mathbf{p}} \mp p_*^0(\mathbf{p})$.

SUMMARY AND DISCUSSION

In the main text, we have integrated over the times of interaction x^0 and y^0 before the Φ -energy p^0 . Instead we may first integrate over p^0 before x^0 and y^0 , and see how the time-boundary effect emerges at $x^0, y^0 = \Im_{\text{in/out}}$. This will be shown in detail in a separate publication.